

# High frequency (>60 GHz), atomic core-level spectroscopy using a high-harmonic generation light source

M. Tanksalvala\*<sup>a</sup>, Anthony Kos<sup>a</sup>, Jacob Wisser<sup>a</sup>, Scott Diddams<sup>b,c,d</sup>, Hans T. Nembach<sup>a</sup>, Justin M. Shaw<sup>a</sup>

<sup>a</sup>Applied Physics Division, National Institute of Standards and Technology, Boulder, CO 80305;

<sup>b</sup>Time & Frequency Division, National Institute of Standards and Technology, Boulder, CO 80305;

<sup>c</sup>Electrical, Computer & Energy Engineering, University of Colorado, Boulder, CO 80309;

<sup>d</sup>Department of Physics, University of Colorado, Boulder, CO 80309

## ABSTRACT

Atomic core-level spectroscopy is an invaluable metrological tool in a wide array of fields, from quantum and materials science to semiconductor metrology. When applied to dynamical systems, it enables the measurement of element- and layer-specific dynamics. While such spectroscopy has been applied widely in conjunction with optical excitation of samples, its combination with a high-frequency microwave excitation is less common; in principle, however, this combination enables *in operando* measurements of devices. Toward this goal, we have developed an instrument that uses an RF frequency comb generator to produce high-frequency microwaves (>60 GHz) that are synchronized to a tabletop, high-harmonic generation light source with <1.1ps timing jitter. This system can be used to study, with element-specificity, the switching behavior of devices at their operating frequency as well as the resonant behavior of devices or novel materials and systems. For instance, by applying an external magnetic field and tuning the microwave frequency to the ferromagnetic resonance in magnetic films, we can perform high-frequency x-ray or extreme ultraviolet detected ferromagnetic resonance (XFMR) spectroscopy. As a demonstration, we measure XFMR of three sample systems (permalloy, CoFe, and a Fe/TaO<sub>x</sub>/Ni multilayer). In the future, we can augment this capability with coherent diffractive imaging to perform high-frequency, resonant spectroscopy with sub-100 nm spatial resolution.

**Keywords:** HHG, EUV, frequency combs, spectroscopy, thin films, interfaces, FMR, XFMR

## 1. INTRODUCTION

Device-level, laboratory-scale, non-destructive, *in operando* metrology of structure and transport is a long-unrealized goal, important across scientific and industrial disciplines from next-generation semiconductor and quantum devices to cutting-edge materials for non-conventional computing. A variety of metrological approaches have been developed to address different aspects of this need. Atomic core-level spectroscopy (e.g., using x-rays to probe a sample) provides the ability to measure, nondestructively and often quantitatively, the composition, structure, and state of the individual elements within a sample.[1,2] When used in conjunction with an excitation, either optical or electrical, it enables the measurement of element- and layer-specific dynamics. For instance, ultrafast demagnetization and photoemission spectroscopic studies have provided insight into fundamental physical processes at the nano-scale.[3-5] On the other hand, using electrical excitation enables studies of processes under real-world conditions. Using very low frequency excitation, slow processes such as dendrite formation within batteries can be investigated.[6] With proper synchronization to the x-ray probing light, higher frequency excitation provides the means to measure resonant behavior of novel device systems and, in principle, transport and switching behavior within active devices.[7,8] Microwave-excited, x-ray-detected measurements provide a promising building block to achieve the overall goal of measuring transport within active devices. Unfortunately, these measurements have not been available in a laboratory setting, being primarily limited to facility-scale sources; furthermore, they often are limited to few-GHz excitation frequencies due to the pulse duration of the x-ray source. Higher-frequency excitations would give access not only to sharper switching pulses for devices, but also to resonant phenomena that are difficult to measure or that do not activate until higher frequencies.[9]

Using these measurements as inspiration, we have developed an instrument that produces high-frequency microwaves (>60 GHz) that are synchronized to a tabletop, femtosecond, high-harmonic generation light source, with <1.1ps timing jitter.[10] Using extreme ultraviolet (EUV) light as an element-specific probe, this instrument can be used to study the switching behavior of devices at their operating frequency, or the resonant behavior of devices or novel materials and

systems. As a demonstration, we perform high-frequency x-ray detected ferromagnetic resonance (XFMR) spectroscopy on three magnetic thin-film samples (permalloy, CoFe, and a Fe/TaO<sub>x</sub>/Ni multilayer). In the future, we can augment this capability with coherent diffractive imaging to perform high-frequency, resonant spectroscopy with sub-100 nm spatial resolution.

## 2. EXPERIMENT APPARATUS

Our instrument is built from a mode-locked Ti:sapphire oscillator operating at ~82 MHz, with a center wavelength around 800 nm. The oscillator seeds an electrical system that generates the microwave excitation and an optical system that ultimately produces the EUV measurement pulse. Importantly, since the same oscillator seeds both processes their outputs are intrinsically synchronized, and the EUV pulses will always impinge on the sample at the same phase of the applied microwaves unless the microwaves are deliberately phase-shifted. With an appropriate phase-shifter, this allows measurement of dynamics over a cycle of the excitation.

The electrical system starts with a photodiode that outputs an electrical pulse train at the oscillator frequency. This pulse train is input into an RF frequency comb generator that produces frequencies exceeding 20 GHz. A pair of YIG-tuned filters select a single tooth of the frequency comb. These filters serve a dual purpose: they also impart a phase shift of the microwaves that depends on how well the selected comb tooth is centered on the filter passband. By detuning the passband slightly, the microwave output does not decrease but the phase can be varied precisely over a cycle. Most of the components have a bandwidth of 8.5 GHz – 12 GHz; we insert frequency multipliers to exceed this range and have seen no evidence that this increases our timing jitter appreciably. After sufficient amplification, the microwaves are delivered to the sample.

The oscillator seeds a regenerative Ti:sapphire amplifier that operates at 3 kHz and can output up to 10 W (3.33 mJ). To perform high-harmonic generation (HHG), this laser is focused into a hollow-core glass capillary filled with a noble gas. In this study, we measured several magnetic thin films whose M-edges lie between 45 eV and 70 eV; to drive phase-matched HHG for these wavelengths we use approximately 0.8 mJ pulse energy and roughly 50000 Pa of Ne gas. After attenuating the driving 800 nm light using a pair of grazing-incidence Ru-coated mirrors and 500 nm-thick Al foils, the EUV light is focused (using a grazing-incidence toroidal mirror) into a ~40 μm diameter spot on the sample. The light that reflects from the sample is re-focused using a second toroid in a 1:1 imaging configuration, reflects from a grazing-incidence grating (500 lines/mm), and the spectrally-resolved beamlets are finally collected on a CCD camera.

To perform XFMR, we fabricated a sample consisting of a lithographically patterned coplanar waveguide with the magnetic material patterned on top of the center conductor. The experiment is configured in the transverse-MOKE geometry, with EUV light incident on the sample near Brewster's angle and a horizontally-oriented electromagnet that applies a magnetic field in the sample plane. In this geometry, the projection of the magnetic moment onto the vertical axis, perpendicular to the plane of incidence, is the detected magnetic state. If the magnetic field changes direction (or if the microwaves are phase-shifted), the intensity of the reflected spectrum will change in proportion to the magnetic state; photon energies that lie near the M-edge of magnetized elements will change intensity dramatically, even exceeding 50% change. When microwaves are applied at or near the ferromagnetic resonance, the spins will precess about the applied field, and by phase shifting the microwaves relative to the EUV pulse, the magnetic signal sinusoidally varies. The amplitude and phase of that oscillation are measured as the applied magnetic field is tuned across the ferromagnetic resonance, thus forming XFMR curves.

## 3. DATA

### Timing Jitter

We first determined the frequency limit of the microwave excitation produced by our instrument. The EUV probe is ~10 fs long, so it provides an intrinsic frequency limitation of ~100 THz, far above any practical limitations of the present instrument. The practical limitations come from two sources: (1) some resonant phenomena decrease in amplitude at higher frequencies, thus decreasing SNR, and (2) the timing jitter between the microwave excitation and the EUV measurement probe will reduce signal when the timing jitter is on the order of one period of the microwave excitation. The former is a matter of SNR and will depend on the sample. To quantify the timing jitter, we performed measurements (see Fig. 1) at frequencies ranging from 8 GHz to 62 GHz, and at all frequencies the timing jitter was <1.1 ps. This timing jitter is on the order of the intrinsic jitter of the sampling oscilloscope, and therefore serves an upper bound rather than a precise measurement. This level of timing jitter supports measurements of 100 GHz or higher, in principle. Note that the

bandwidth of the sampling oscilloscope was 40 GHz (less than most of our measurements in Fig. 1). Along with a bandpass filter in our setup whose bandwidth was also exceeded by a few GHz, this leads to the distortion observed in the 62 GHz trace. This distortion is not a limitation, since we can replace the bandpass filter with a commercially available component of an appropriate frequency range.

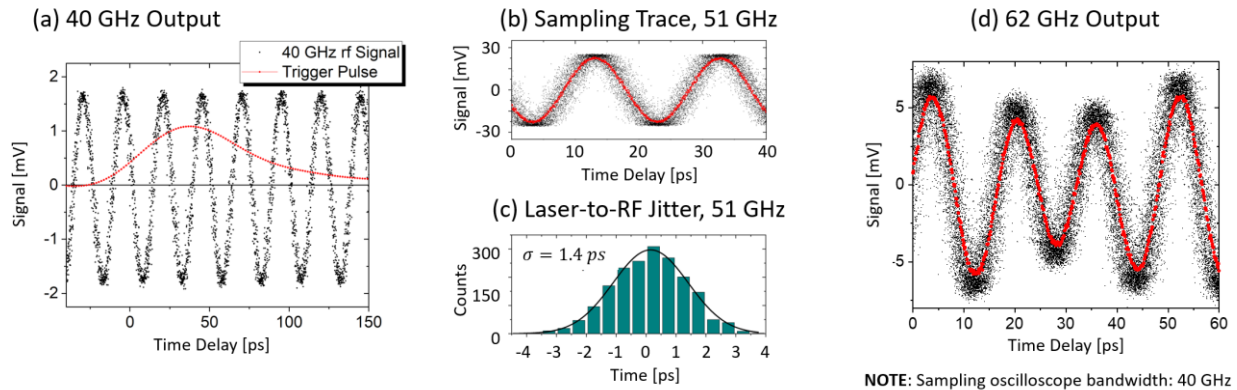


Figure 1. Sampling oscilloscope traces of microwave excitation up to >60 GHz. (a) Sampling scope trace of a 40 GHz excitation (black) and from a fast photodiode (red) that views the 800 nm driving laser. (b) Sampling scope trace of a 51 GHz excitation. The characteristic of timing jitter appears in this plot, where the noise near the extrema of the sine wave disappears, indicating that the fuzziness of the trace provides a measurement of the timing jitter. (c) Histogram of the timing jitter of the 51 GHz trace, showing 1.4 ps of jitter. Factoring in the jitter of the sampling oscilloscope itself, this provides an estimate of <1.1 ps timing jitter between the EUV and microwaves. (d) Sampling oscilloscope trace of 62 GHz excitation. The low SNR and distortion are artifacts resulting from exceeding the bandwidth of the sampling oscilloscope (40 GHz) and a bandpass filter within the system (~59 GHz).

### X-Ray Detected Ferromagnetic Resonance (XFMR)

We next applied this system to perform field-swept x-ray detected ferromagnetic resonance (XFMR) spectroscopy measurements. With the maximum magnetic field we can apply in our current setup (approximately  $\mu_0 H = 150$  mT), the ferromagnetic resonance is near 8.5 GHz for permalloy and a Fe/TaO<sub>x</sub>/Ni multilayer, and near 17 GHz for a CoFe sample. Therefore, we applied an 8.5 GHz excitation to permalloy and the multilayer sample, and 17 GHz to CoFe. The XFMR results are shown in Fig. 2.

The XFMR measurement of the Ni and Fe spins within Ni<sub>80</sub>Fe<sub>20</sub> (permalloy), shown in Fig. 2a, demonstrates the ability to measure full XFMR curves individually for the different elements within the sample. The measurement of amplitude (black) and phase (blue) are shown as points, and the fit to the susceptibility derived from the Landau-Lifshitz equation is shown as solid lines of the respective color. The quality of the fit is good enough to lend confidence to the proper function of the instrument, as is the agreement of the XFMR amplitude traces with an *in situ* inductive FMR of the same sample.

The trace for CoFe shown in Fig. 2b also shows agreement between FMR and XFMR. The two resonance peaks appear at the same locations in both FMR and XFMR, leading us to believe that they are due to inhomogeneity within the sample.

The multilayer sample shown in Fig. 2b is designed to electrically isolate the two magnetic layers, and highlights the ability to extract element- or layer-specific dynamics. When we apply 8.5 GHz excitation with an applied magnetic field near  $\mu_0 H = 50$  mT (Fe resonance), the precession amplitude of the Fe spins is larger than that of the Ni spins. When we apply the same excitation near  $\mu_0 H = 125$  mT (Ni resonance), the situation is reversed and the Ni precession amplitude is larger. There is a visible relative phase between the respective oscillations that lends insight into the coupling mechanisms (if any) between the two layers. In the future, we can measure the progression of that phase difference across the resonances, and thereby quantitatively determine the coupling mechanisms in scientifically and technologically interesting magnetic multilayer systems.

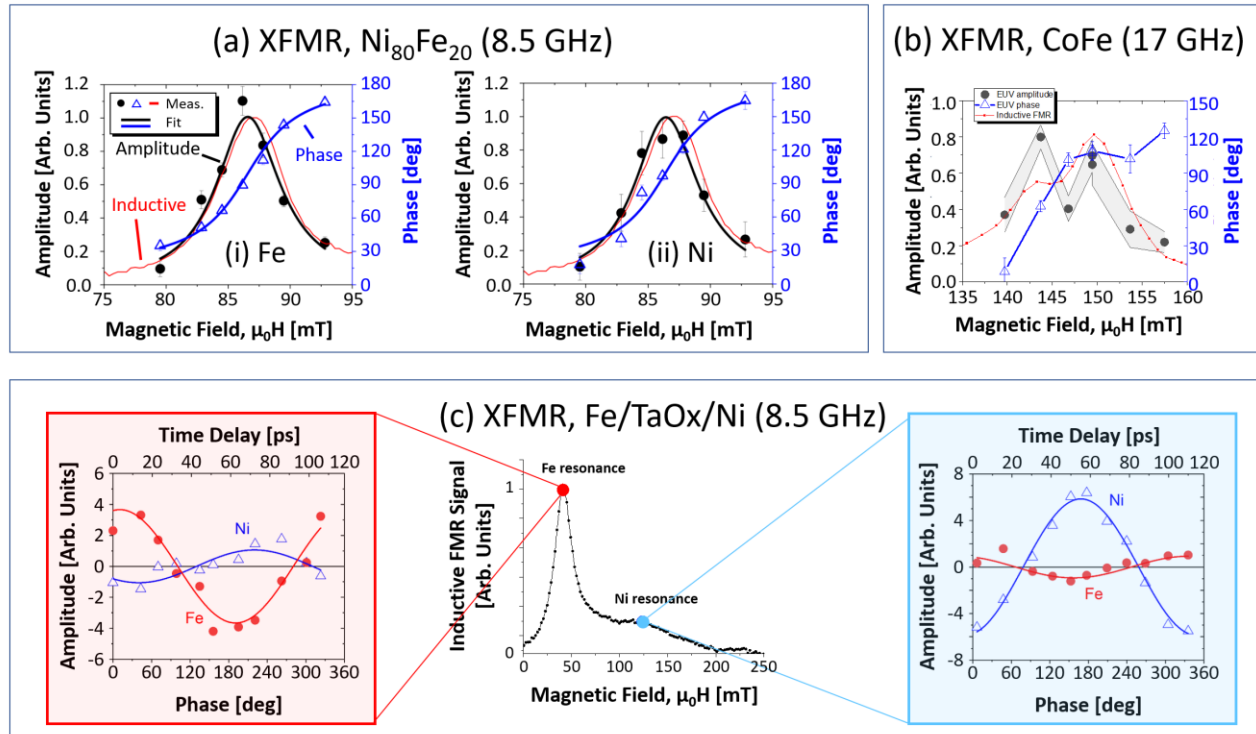


Figure 2. High-frequency, x-ray detected ferromagnetic resonance (XFMR) measurements. (a) Measured XFMR traces of a NiFe alloy (Permalloy). The measured XFMR amplitude is shown as black dots and the phase as blue triangles. The two elements appear to exhibit identical dynamics, as expected (the traces match each other). The amplitude and phase are simultaneously fit to the susceptibility derived from the Landau-Lifshitz equation, and these fits are shown as solid lines in their respective colors. For verification, the same sample was also measured using an *in situ* inductive FMR setup, and the resulting trace is shown in red. (b) Measured XFMR traces of a CoFe alloy, performed with 17 GHz excitation. (c) Measured spin precessions of an Fe/TaO<sub>x</sub>/Ni magnetic multilayer sample. Because the Fe and Ni are electrically isolated with only weak dipole coupling, they have different resonant fields. When the resonant field for Fe is applied, the Fe spins are observed to precess with greater amplitude than the Ni spins, and similarly at the Ni resonance. The visible phase shift between the two oscillations can lend insight into the coupling mechanisms, if any, between the two layers.

#### 4. CONCLUSIONS

We have developed an instrument that can perform high-frequency (>60 GHz) resonant studies, measured with extreme ultraviolet light (EUV) to provide element- and layer-specific information. This laboratory-scale instrument uses high-harmonic generation (HHG) to generate an EUV measurement pulse and uses an RF frequency comb generator to produce a microwave excitation that is intrinsically synchronized to the EUV pulses with <1.1ps timing jitter. We applied this instrument to perform high-frequency x-ray detected ferromagnetic resonance (XFMR) spectroscopy on permalloy (8.5 GHz), CoFe (17 GHz), and a Fe/TaO<sub>x</sub>/Ni multilayer (8.5 GHz, with element-specific dynamics). This instrument can in the future measure scientifically and technologically interesting and industrially relevant samples, including spintronic and semiconductor devices. Furthermore, by combining this with the high spatial resolution afforded by coherent diffractive imaging, it has the possibility to image, nondestructively and with element-specificity, transport within novel materials as well as the dynamics of devices switching at their operating frequencies.

#### ACKNOWLEDGEMENTS

The authors are grateful to Henry Kapteyn, Margaret Murnane, and Tom Silva for valuable discussions and advice, and to Dmitry Zusin and Christian Gentry for developing the multilayer reflectivity calculating code. MT and JW acknowledge

funding support from the National Research Council (NRC) Post-Doctoral Fellowship program. HTN acknowledges support through the NIST cooperative agreement 70NANB18H006 with the University of Colorado Boulder.

## REFERENCES

- [1] M. Holler, M. Guizar-Sicairos, E.H.R. Tsai, *et al.* "High-resolution non-destructive three-dimensional imaging of integrated circuits." *Nature* 543.7645 (2017): 402-406.
- [2] M. Tanksalvala, C.L. Porter, Y. Esashi, *et al.* "Nondestructive, high-resolution, chemically specific 3D nanostructure characterization using phase-sensitive EUV imaging reflectometry". *Science Advances* 7.5 (2021): eabd9667.
- [3] S. Mathias, C. La-O-Vorakiat, P. Grychtol, *et al.* "Probing the timescale of the exchange interaction in a ferromagnetic alloy." *Proceedings of the National Academy of Sciences* 109.13 (2012): 4792-4797.
- [4] E. Turgut, D. Zusin, D. Legut, *et al.* "Stoner versus Heisenberg: Ultrafast exchange reduction and magnon generation during laser-induced demagnetization." *Physical Review B* 94.22 (2016): 220408.
- [5] Z. Tao, C. Chen, T. Szilvási, *et al.* "Direct time-domain observation of attosecond final-state lifetimes in photoemission from solids." *Science* 353.6294 (2016): 62-67.
- [6] V. Yufit, F. Tariq, D.S. Eastwood, *et al.* "Operando visualization and multi-scale tomography studies of dendrite formation and dissolution in zinc batteries." *Joule* 3.2 (2019): 485-502.
- [7] D.A. Arena, E. Vescovo, C.-C. Kao, *et al.* "Combined time-resolved x-ray magnetic circular dichroism and ferromagnetic resonance studies of magnetic alloys and multilayers (invited)," *Journal of Applied Physics* 101.9 (2007): 09C109.
- [8] G. van der Laan, and T. Hesjedal. "X-ray detected ferromagnetic resonance techniques for the study of magnetization dynamics." *Nuclear Instruments and Methods in Physics Research Section B: Beam Interactions with Materials and Atoms* 540 (2023): 85-93.
- [9] J.M. Shaw, H.T. Nembach, and T.J. Silva. "Determination of spin pumping as a source of linewidth in sputtered Co<sub>90</sub>/Fe<sub>10</sub>/Pd multilayers by use of broadband ferromagnetic resonance spectroscopy." *Physical Review B—Condensed Matter and Materials Physics* 85.5 (2012): 054412.
- [10] M. Tanksalvala, A. Kos, J. Wisser, *et al.* "Element-specific high-bandwidth ferromagnetic resonance spectroscopy with a coherent extreme-ultraviolet source." *Physical Review Applied*, 21.6 (2024): 064047.